NATIONAL LABORATORY OF THE ROCKIES

Development of Biofuel and Bioenergy Processes for Photosynthetic CO_2 Assimilation

Cooperative Research and Development Final Report

CRADA Number: CRD-18-00765 (Project 2)

NLR Technical Contact: Lieve Laurens

The National Laboratory of the Rockies is a national laboratory of the U.S. Department of Energy, Office of Critical Minerals and Energy Innovation, operated under Contract No. DE-AC36-08GO28308.

This report is available at no cost from the National Laboratory of the Rockies (NLR) at www.nlr.gov/publications.

Technical Report
NLR/TP-2700-98764
February 2026

NATIONAL LABORATORY OF THE ROCKIES

Development of Biofuel and Bioenergy Processes for Photosynthetic CO_2 Assimilation

Cooperative Research and Development Final Report

CRADA Number: CRD-18-00765 (Project 2)

NLR Technical Contact: Lieve Laurens

Suggested Citation
Laurens, Lieve. 2026. *Development of Biofuel and Bioenergy Processes for Photosynthetic CO_2 Assimilation: Cooperative Research and Development Final Report, CRADA Number CRD-18-00765 (Project 2).* Golden, CO: National Laboratory of the Rockies. NLR/TP-2700-98764. https://www.nlr.gov/docs/fy26osti/98764.pdf.

The National Laboratory of the Rockies is a national laboratory of the U.S. Department of Energy, Office of Critical Minerals and Energy Innovation, operated under Contract No. DE-AC36-08GO28308.

This report is available at no cost from the National Laboratory of the Rockies (NLR) at www.nlr.gov/publications.

Technical Report
NLR/TP-2700-98764
February 2026

National Laboratory of the Rockies
15013 Denver West Parkway
Golden, CO 80401
303-275-3000 • www.nlr.gov

NOTICE

This work was authored by the National Laboratory of the Rockies for the U.S. Department of Energy (DOE), operated under Contract No. DE-AC36-08GO28308. Funding provided by the U.S. Department of Energy Office of Energy Efficiency and Renewable Energy Bioenergy Technologies Office. The views expressed herein do not necessarily represent the views of the DOE or the U.S. Government.

This work was prepared as an account of work sponsored by an agency of the United States Government. Neither the United States Government nor any agency thereof, nor any of their employees, nor any of their contractors, subcontractors or their employees, makes any warranty, express or implied, or assumes any legal liability or responsibility for the accuracy, completeness, or any third party's use or the results of such use of any information, apparatus, product, or process disclosed, or represents that its use would not infringe privately owned rights. Reference herein to any specific commercial product, process, or service by trade name, trademark, manufacturer, or otherwise, does not necessarily constitute or imply its endorsement, recommendation, or favoring by the United States Government or any agency thereof or its contractors or subcontractors. The views and opinions of authors expressed herein do not necessarily state or reflect those of the United States Government or any agency thereof, its contractors or subcontractors.

This report was produced when the laboratory operated as the National Renewable Energy Laboratory (NREL). The laboratory is now the National Laboratory of the Rockies (NLR).

This report is available at no cost from the National Laboratory of the Rockies (NLR) at www.nlr.gov/publications.

U.S. Department of Energy (DOE) reports produced after 1991 and a growing number of pre-1991 documents are available free via www.OSTI.gov.

Cover photos (clockwise from left): Josh Bauer, National Laboratory of the Rockies 61725; Visualization from National Laboratory of the Rockies Insight Center; Getty-181828180; Agata Bogucka, National Laboratory of the Rockies 91683; Dennis Schroeder, National Laboratory of the Rockies 51331; Werner Slocum, National Laboratory of the Rockies 67842.

National Laboratory of the Rockies prints on paper that contains recycled content.

Cooperative Research and Development Final Report

Report Date: November 11, 2025

In accordance with requirements set forth in the terms of the CRADA agreement, this document is the CRADA final report, including a list of subject inventions, to be forwarded to the DOE Office of Scientific and Technical Information as part of the commitment to the public to demonstrate results of federally funded research.

Parties to the Agreement: ExxonMobil Technology and Engineering Company

CRADA Number: CRD-18-00765 (Project 2)

CRADA Title: Development of Biofuel and Bioenergy Processes for Photosynthetic CO_2 Assimilation

Period of Performance: 4/9/2019 - 6/30/2024

Responsible Technical Contact at NLR:

Lieve Laurens | Lieve.Laurens@nlr.gov

Name and Email Address of POC at Company:

Ruby Carrillo | Leticia.R.Carrillo@exxonmobil.com

Sponsoring DOE Program Office(s):

Office of Energy Efficiency and Renewable Energy (EERE), Bioenergy Technologies Office

Joint Work Statement Funding Table showing DOE commitment:

No NLR Shared Resources.

Executive Summary of CRADA Work:

In order to fully exploit algae carbon assimilation for fuels, a preqrequisite is high photosynthetic efficiency and carbon conversion to fuel precursors. In the context of this collaborative project between NLR and EMRE we aim to address aspects of both the biological constraints around photosynthesis-driven carbon assimilation flux as well as elements that bridge the gap between laboratory cultivation and meaningful outdoor deployment, building on the unique capabilities of NLR and EMRE's algae bioengineering teams. The goal of this work is to improve our understanding of key cellular biochemistry, mass cultivation, and biomass conversion constraints that presently limit the potential bio-oil yield. The proposed first phase of this work will focus on biomass growth improvements by testing hypotheses for alleviating identified metabolic and photophysiological bottlenecks. The results of this work could inform decisions by stakeholders (e.g., industry, community, investors) on the design and deployment of a sustainable biofuel supply chain from algae.

This report is available at no cost from the National Laboratory of the Rockies (NLR) at www.nrel.gov/publications.

CRADA benefit to DOE, Participant, and US Taxpayer:

Uses the laboratory's core competencies

Summary of Research Results:

Task 1: Develop a genetic engineering approach for photosynthetic improvement through a comparative study of the photophysiological and carbon flux differences between the two variants of *P. celeri* to identify a metabolic basis for improved utilization of light energy and distribution of fixed carbon.

Planned activities:

- Carry out comparative 'omics' analysis of the *P. celeri* improved cultivar relative to sister cultivars (from the same enrichment culture), including geonomics, transcriptomics, metabolomics and proteomics analyses to elucidate major changes underpinning rapid, inter-cultivar growth rate improvements. The initial goal will be to determine whether the specific enzymes and regulators, in particular photosynthetic proteins, found in the prior study of growth variants of *Synechoccus* play a similar role in *P. celeri* variants. Reverse genetics on these targets will be included in Task 2 and mature bioinformatics pipelines will be used to rapidly determine additional targets for metabolic engineering to be carried out in Task 2.
- Analyze CO_2 uptake between the two *P. celeri* strain cultivars, using customized membrane inlet mass spectrometry (MIMS) instrumentation to identify carbon uptake processes supporting the more rapid biomass accumulation phenotype observed. This system will be upgraded with a monochromator to include an analysis of the action spectrum of photosynthesis, where physiological activity is measured (in this case CO_2 and O_2 evolution rates) for different wavelengths of light.
- Assess metabolic carbon assimilation by developing CO_2-based fluxomics model for carbon pathways in *P. celeri*, identifying metabolic bottlenecks. Seek to understand the low lipid basal productivity of *P. celeri*, and to identify any differences in the two variants of *P. celeri.*

The outcome of task 1 will be a number of high-impact journal articles describing the fundamental photosynthetic underpinning of fast-growing algae. Where appropriate to commercialization, intellectual property filings will precede the publication.

This report is available at no cost from the National Laboratory of the Rockies (NLR) at www.nrel.gov/publications.

Task 1 Results:

To support the development of strain improvement strategies and probe photosynthetic carbon assimilation in select *P. celeri* algae cultivars, we carried out detailed physiological comparison experiments.

The experimental system was centered around two variants of *Picochlorum celeri* as representatives of high-yielding, fast growing algae, with the idea that fundamental mechanisms elucidated with these comparisons would be transferable to other algae and likely terrestrial plants for improved improved autotrophic carbon assimilation rates. The *P. celeri* strain designated as TG2 has one of the fastest reported specific growth rates for a microalgae species of 0.34 h−1 (roughly translating to a 2 h doubling time) after rapid acclimation to high irradiance (1000 µmol m−2 s−1)(*1–3*). High light selection also produced a closely related *P. celeri* isolate, TG1, that presents a significantly lower specific growth rate than TG2 of 0.22 h−1. In combination, these two strains represent a powerful study system to elucidate genetic and metabolic diel carbon allocation control mechanisms.

The objective of this work was to elucidate the genetic and metabolic regulating mechanisms governing growth, light response, and composition differences of two isolates, or variants, of *P. celeri*, TG1 and TG2, whose genomes are very closely related, but exhibit a consistently different physiological, and transcriptional phenotype. High-light (HL) stress, under uniquely controlled environmental conditions, was used to elicit the fast growth and high starch accumulation phenotype, in TG2 and TG1, respectively. Closely coordinated transcriptomics with fluxomics analysis allows for deconvoluting an extensive covariance matrix of the physiological response to identify a global regulatory mechanism. We then demonstrated the impact of the identified regulator on the global genetic and photosynthetic carbon allocation phenotype of an engineered strain that may have implications towards a translatable central control system in higher plants

To specifically look for unique and differential gene expression behavior in the light response of both isolates, several different analyses were carried out to isolate the interaction effect between light and strain for the 1 h time point. The majority of significantly changed transcript levels after 1 h in were down regulated relative to the LL levels in each of the wild type strains (Fig. 1.1A, B). There was not a single transcript which was changed in the opposite direction between TG1 and TG2 after applying the same fold change and significance filtering thresholds (Fig. 1.1C). With a carefully-designed likelihood ratio test on the full transcriptome, we were able to identify several transcripts that exhibited a statistically significant interaction effect in their expression response to high light transition and genetic background (Fig. 1.1D). The single most significant gene identified in this analysis (EMRE3EUKT4064225), was annotated as a transcription factor encoding a homolog of late elongated hypocotyl/circadian clock associated like (LHY/CCA) and was strongly separated from the rest of the transcriptome.

This report is available at no cost from the National Laboratory of the Rockies (NLR) at www.nrel.gov/publications.

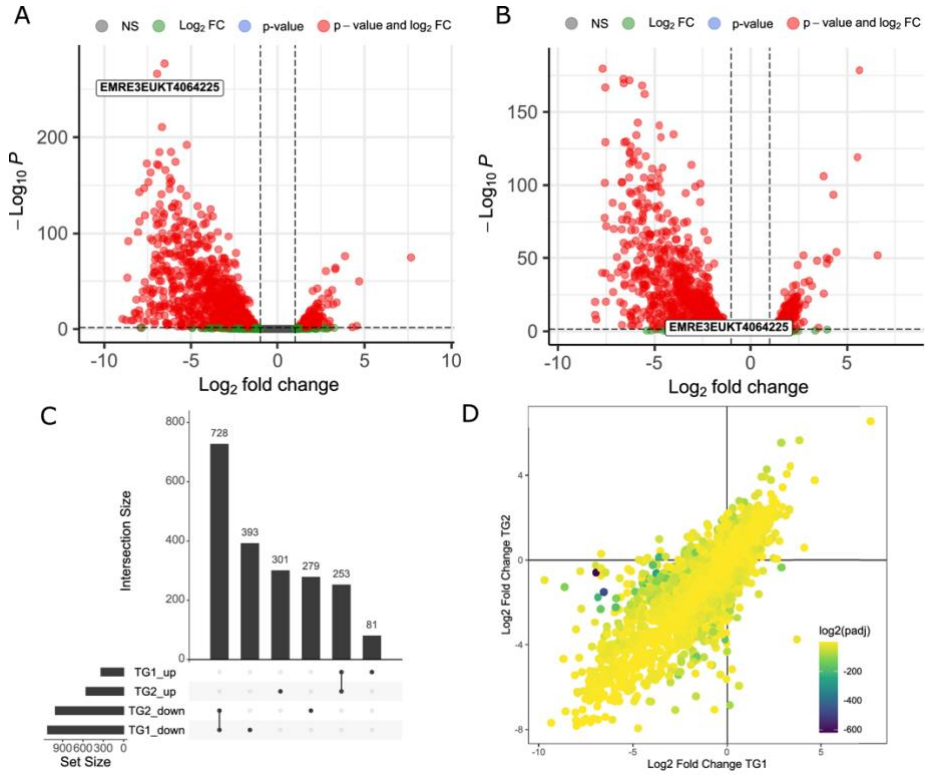

Fig. 1.1. Gene expression variation between TG1-WT and TG2-WT upon exposure to high light intensity, based on RNA-seq data collected from wild type P. celeri cultures after 1 h of exposure to HL conditions following acclimation to LL (T = 0). Changes in transcript abundances of (A) TG1 and (B) TG2 cultures expressed as Log2 of the fold changes between 1 h high light and steady state low light growth. Dashed lines represent threshold values for fold change and p-values (L2FC(1) and 0.05, respectively) used to identify significant gene sets, as determined by a two-sided Wald test using Benjamini–Hochberg multiple testing adjustment. The putative CCA1 transcript is labeled in each with its transcript ID number, and not significant (NS) genes colored in gray. C Comparison of significant differentially expressed gene sets between TG1 and TG2. The sets identified in above panels were separated into up or down regulated groups and all combinations of comparison are represented in the lower matrix with the number of members shown in the above bars. D Statistical analysis to deconvolute P. celeri TG1 and TG2 isolates' transcriptome. The results of a two-sided likelihood ratio test determining the significance of each gene to a model isolating the interaction term between high light exposure time and strain is displayed as color scaled p-values over the fold change observed for each gene. All data shown are derived from independent biological replicate cultures (n = 3)

The translated protein sequence indicated a close relationship with *A. thaliana* homologs for CCA1 and LHY containing the conserved domain related to the SANT family of MYB-like DNA binding sequences hereafter referred to as *Picochlorum* CCA1. The variation in TG2 and TG1 CCA1 gene transcription may be in part due to sequence variant sites apparent in an alignment of the genomic loci, including a 9 bp insertion in the TG2 promoter region 590 bp upstream of the translation start site as well as a deletion and insertion event within 170 bp downstream of the stop codon, which may lie beyond the 3′ UTR as RNA-seq read data coverage extends to ~165 bp. The coding sequence of the TG1 CCA1 gene contains up to 20 predicted non-synonymous sequence variants with respect to the TG2 genomic locus.

This report is available at no cost from the National Laboratory of the Rockies (NLR) at www.nrel.gov/publications.

The identification of metabolic control points over carbon allocation from the photosynthetic source across the CBB and central carbon metabolism is important to define the fate of fixed carbon. Accurate estimation of intracellular fluxes in the metabolic network (e.g., through Instationary metabolic flux analysis (INST-MFA15, or fluxomics with 13C stable isotope tracking of metabolic carbon) is a critical component of carbon allocation optimization by identifying metabolic bottlenecks in algae and plants (*4*, *5*). Using advanced MFA methods, we were able to assess metabolic carbon assimilation by developing CO_2-based fluxomics model for carbon pathways in *P. celeri*, identifying metabolic bottlenecks.

The remainder of the comparative discussion is included in the task 2 descriptions, where genetically engineered cultivars of *P. celeri*, where the *Picochlorum* CCA1 from the TG2 cultivar was transferred to the TG1 cultivar, and continued comparative analyses are reported in the engineered (TG1MYB99) cultivar relative to the respective parental strains.

Task 2: Develop an approach that allows for testing the novel hypotheses for genetic improvement of productivity and carbon assimilation in algae species translatable to strains for outdoor deployment.

Planned activities:

- Develop genetic engineering tools for P. celeri building on established transformation and gene editing protocols developed under existing projects at NLR for a different Picochlorum species. Evaluate the efficacy of heterologous control elements in bypassing host regulation.
- Identify key genetic components from Task 1 global 'omics' comparisons to target in a dedicated genetic engineering approach and test whether modulation of these targets show biomass productivity improvements in P. celeri after conducting forward and reverse genetics to verify target gene functionality and ultimately to increase the productivity of even the fastest-doubling cultivar.

The outcome of task 2 will be published journal articles describing improved understanding of the basis of fast growing algae, and aspects of the fundamental metabolic underpinning of what drives algal biomass productivity. will precede the publication. The work plan included here directly addresses the fundamental questions on the molecular basis for growth rate determination may elucidate mechanisms that can be translated and tool development that can be ultimately transferred to species amenable to large-scale farming operations.

Task 2 Results:

A secondary goal of the work above focused on elucidating with genetic engineering the specific function of the selected targets. The identified key genetic component (EMRE3EUKT4064225, homolog of late elongated hypocotyl/circadian clock associated like (LHY/CCA)) from Task 1 global 'omics' comparisons was targeted in a dedicated genetic engineering approach and test whether modulation of these targets show biomass productivity improvements in *P. celeri* after conducting forward and reverse genetics to verify target gene functionality and ultimately to increase the productivity of even the fastest-doubling cultivar.

This report is available at no cost from the National Laboratory of the Rockies (NLR) at www.nrel.gov/publications.

We used established genetic engineering tools for *P. celeri* to test the impact of the genome-wide regulatory CCA1 function in *P. celeri* as related to both growth and carbon allocation dynamics by creating a genetically engineered variant of TG1 with the TG2-WT CCA1 gene elements transformed into a TG1-WT background using an expression vector containing the TG2 CCA1 coding sequence under control of the TG2 native promoter and terminator regions. The cell line with the highest specific growth rate in high-light conditions was selected from a screen of transformants for further analysis and was designated TG1-MYB99.

A four-hour time course RNA sampling during transition from LL to HL was conducted to determine the transcriptional regulatory alterations in the TG1-MYB99 strain. All strains demonstrated a biphasic acclimation to the increased light intensity, with the largest shift in gene expression occurring 30 min and 1 h after HL and gene expression trending back towards LL levels by the fourth hour (Fig. 2.2A). A persistent down-regulation in the TG1-WT cultures was observed, while TG2-WT maintained the intermediate level observed under LL illumination (Fig. 2B). The time course of CCA1 gene expression dynamics of the TG1-MYB99 strain confirms the successful transfer and expression of TG2 gene elements, starting with high-expression levels as for WT TG1 and upon HL transition shifting to follow the continued high expression as observed for TG2 (Fig. 2.2B). The global transcriptomics response over the 4 h time course similarly positions the TG1-MYB99 strain as intermediate between TG1 and TG2, with a significant fraction of the transcriptome following closely the expression patterns observed in TG2 (Fig. 2.2C). Over-representation statistical analysis of the set of 49 genes that closely matched CCA1 expression dynamics between the cell lines implicated important functions related to biotin metabolism (fatty acid biosynthesis, amino acid catabolism), broad central carbon metabolism, and circadian rhythms (Fig. 2.2D).

This report is available at no cost from the National Laboratory of the Rockies (NLR) at www.nrel.gov/publications.

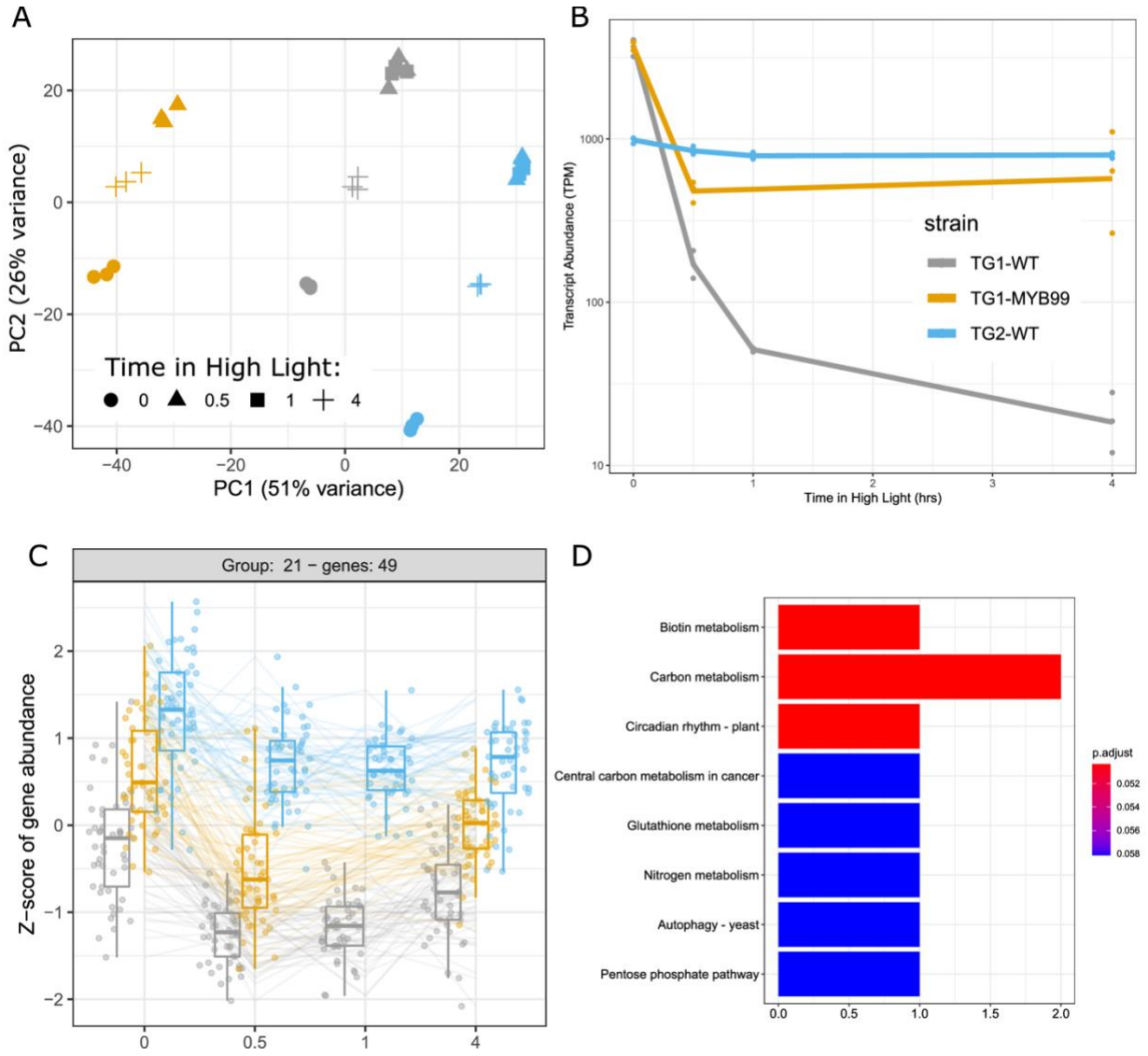

Fig. 2.2. Transcriptional responses of *Picochlorum celeri* TG1 and TG2 isolates and engineered TG1-MYB99 strain, in response to high intensity light shift; (A) The relative position of each sample is displayed based on a principal component analysis scores plot of the regularized log transform data of the 500 most highly expressed transcripts. (B) CCA1 transcriptional dynamics over the acclimation time course. Relative transcript levels were computed following alignment to a reference with a single CCA1 and therefore represent the total pool of TG1 and TG2 transcript isoforms. (C) Time course transcript dynamics of genes clustered based on their similarity to CCA1 expression are displayed by their deviation from median transcript levels of the cluster across the time course with boxplots representing distributions of expression level variances for genes averaged from independent biological replicate cultures (n = 3) centered on the median with lower and upper bounds on the 25th and 75th percentiles, respectively. Lower and upper whiskers indicate minimum and maximum values up to 1.5 times interquartile range in each direction. The corresponding bar plot (D) of enriched functional annotation categories indicates the number of genes with each annotation type and colored by the significance of their over-representation compared to the remaining background genome as computed using a hypergeometric distribution with Benjamini–Hochberg multiple testing adjustment.

This report is available at no cost from the National Laboratory of the Rockies (NLR) at www.nrel.gov/publications.

To assess the respective biomass composition response to light transition, we quantified the primary macromolecular biochemical composition of harvested algal biomass after acclimation to low or high light. Carbon allocation varied dramatically between the cell lines in response to HL conditions, with TG1-WT accumulating as much as 44.9% of its total biomass as carbohydrate, while TG2-WT only reached 16.0% after 48 h of growth in HL. The TG1-MYB99 mutant line cells, remarkably, apportioned over 56% of their biomass to carbohydrate content after the same 48-h acclimation period to HL growth.

To quantify metabolite fluxes through central nodes of carbon assimilation and storage, we applied ^{13}C labeling enabled INST-MFA of TG1 and TG2, and the TG1-MYB99 mutant. This quantitative analysis aims to elucidate key differences in metabolism. Because ^{13}C-labeled CO_2 is challenging to introduce in an immediate and step-change manner (instantaneous change to ^{13}C from ^{12}C for subsequent carbon fixation) that allows for following the ^{13}C tracer over a time course[15], we used a bolus of ^{13}C labeled bicarbonate (1 g L^{-1} $NaH^{13}CO_3$) in a series of physiologically-controlled experiments. To prevent metabolite leakage by quenching methods such as cold methanol quenching, we rapidly filtered cells and quenched in a liquid N2 bath within 10 s of the timepoints. The same metabolic network was used for all three strains and includes compartmentalization and dilution parameters to account for inactive metabolite pools or metabolite channeling, and the INCA 2.0 software package was used to calculate the flux values based on the time course labeling data and solved for the biomass composition. The fitted models estimated CO_2 uptake from the sink demands and was not supplied as an input parameter. TG1, TG1-MYB99, and TG2 had a CO_2 uptake of 5.96, 6.99, and 9.59 mmol g biomass^{-1} h^{-1} respectively.

This report is available at no cost from the National Laboratory of the Rockies (NLR) at www.nrel.gov/publications.

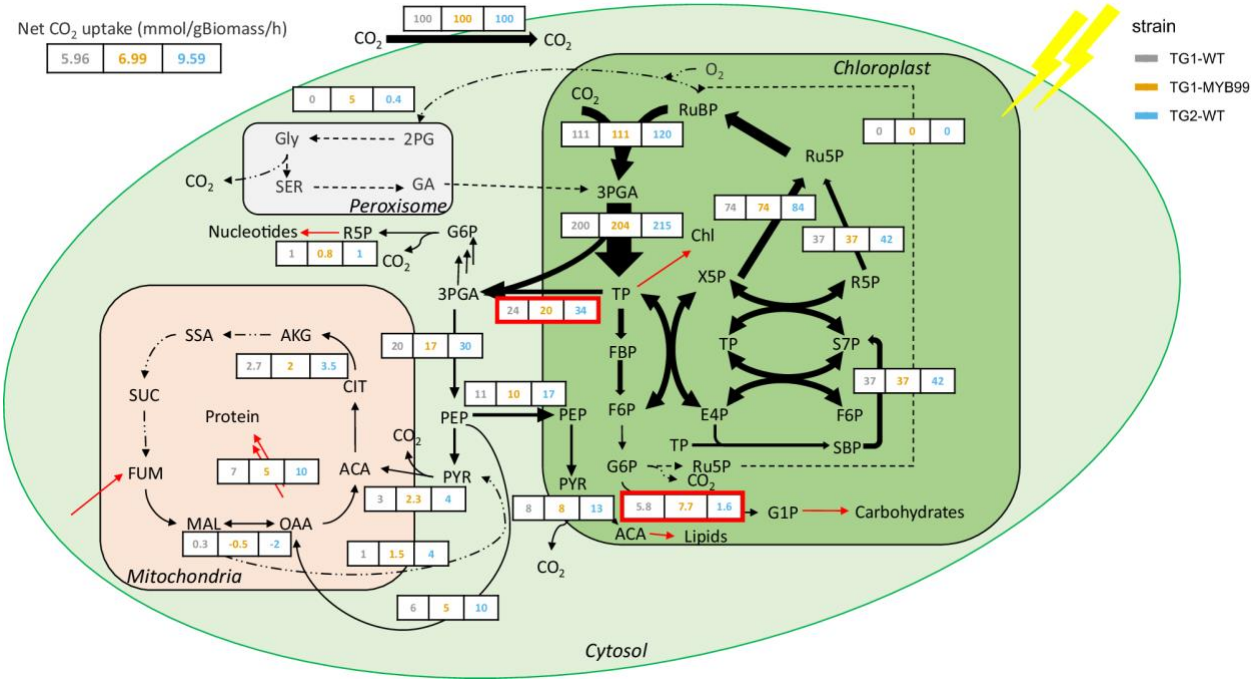

Fig. 2.3. Flux maps determined in TG1, TG1-MYB99, and TG2 under continuous high light conditions (1,000 µE); For each reaction shown, the net fluxes are normalized to 100 units of CO2 taken up. All flux values and confidence intervals are given in Supplementary Data 4. Estimated net CO2 uptake rates for TG1, TG1-MYB99, and TG2 are 5.96, 6.99, and 9.59 mmol gBiomass-1 h-1 respectively (derived from flux models, using n = 3 biological replicated experiments). Ribulose 1,5-bisphosphate (RuBP), 3-phosphoglycerate (3PGA), Triose phosphate (TP), Fructose 1,6-bisphosphate (FBP), Fructose 6-phosphate (F6P), Glucose 6-phosphate (G6P), Glucose 1-phosphate (G1P), Ribulose 5-phosphate (Ru5P), Erythrose 4-phosphate (E4P), Ribose 5-phosphate (R5P), Xylulose 5-phosphate (X5P), Sedoheptulose-7-phosphate (S7P), Sedoheptulose-1,7-bisphosphate (SBP), Phosphoenolpyruvate (PEP), Acetyl-CoA (ACA), Pyruvate (PYR), Glycine (Gly), Serine (SER), 2-phosphoglycolate (2PG), Glycolic acid (GA), Citrate (CIT), Alpha-ketoglutarate (AKG), Succinic semialdehyde (SSA), Succinate (SUC), Fumarate (FUM), Malate (MAL), Oxaloacetate (OAA). Black arrows represent intracellular flux while red arrows represent fluxes to/from biomass sink. The width of the black arrows is indicative of the magnitude of the flux. The red boxes highlight reactions catalyzed by phosphoglucomutase (PGM) and triose phosphate transporter (TPT3) which are implicated in the differing biomass composition phenotypes.

This report is available at no cost from the National Laboratory of the Rockies (NLR) at www.nrel.gov/publications.

TG1 and TG1-MYB99 have a high carbohydrate content which is consistent with the higher flux from F6P in the chloroplast to G6P followed by conversion to G1P and subsequently carbohydrates compared to TG2. The normalized flux from 3PGA as the first product formed after carbon fixation to F6P is not significantly different in the three strains, and a flux difference is only observed in subsequent conversion of F6P to carbohydrates. The conversion of F6P to G6P is catalyzed by the reversible G6P isomerase (EMRE3EUKT4065295) followed by transfer of the phosphate group to position 1 to form G1P catalyzed by phosphoglucomutase (EMRE3EUKT4067541). This is subsequently converted to ADPG by G1P-adenylyl-transferase (EMRE3EUKT4064735, EMRE3EUKT4063059). Transcriptomics analysis suggests that the expression of these enzymes is at least 2-fold higher in TG1 and TG1-MYB99 compared to TG2. This higher expression contributes to the higher flux to carbohydrates in these strains and may suggest that their expression is co-regulated. Expression of PGI and G1P adenylyl-transferase is similar in both TG1 and TG1-MYB99 whereas, in the case of PGM, TG1 has ~2.5-fold higher expression while TG1-MYB99 has a ~4 fold higher expression compared to TG2. This indicates that CCA1 expression further increases carbohydrate accumulation through the control over PGM.

The distinct biomass composition and metabolic demands for these strains, including cellular ATP and NADPH demands, were calculated based on the known metabolic reactions. Linear electron flow (LEF) produces ATP/NADPH in the ratio 1.29 based on the coupled electron-proton reactions that power ATP synthase to generate 3 ATP per 14 protons pumped53. The CBB cycle, on the other hand, requires a higher demand for ATP/NADPH in the ratio 1.554. This imbalance in production and consumption has been suggested as a point of engineering in photosynthesis and forms the basis of the argument that cyclic electron flow (CEF), or an alternative flux of electrons to generate more ATP, is important to balance the ATP/NADPH synthesis and consumption.

The ATP/NADPH ratio is of great importance since an imbalance between the synthesis and consumption of ATP and NADPH is directly linked to photosynthesis. We leveraged the detailed information regarding ATP and NADPH cofactor requirements defined by the INST-MFA flux modelling results to estimate the total energy metabolite demands by each cell line under high light conditions. This analysis showed that TG2 consumes ATP/NADPH in the ratio of 1.58 whereas this number is 1.71 and 1.69 for TG1 and TG1-MYB99 respectively. As the demands on each of these energy carrier pools are linked to different mechanisms in photosynthetic energy balancing, we conducted photophysiology experiments to enable the characterization of the electron flow.

Acclimation responses of the photosynthetic apparatus and related mechanisms can often underly the ability of photoautotrophs to resist abiotic stresses including excessive light intensities. P. celeri TG1 and TG2 cells exhibited remarkably low non-photochemical quenching (NPQ) response after acclimation to high light, and particularly when measured using a pulse amplitude modulated (PAM) fluorometry instrument under 1000 µE actinic light. We developed custom protocols using a fast repetition rate fluorometer (FRRf) that could deliver much higher actinic and saturating pulse light intensities to induce quenching responses and allowed accurate interpretations based on fully activated NPQ. The requirement for this unusually high light intensity regime was validated by remarkably low NPQ for each strain around the range of 0.5, compared to plants such as *A. thaliana* reaching over 2.0 on the classically determined scale.

This report is available at no cost from the National Laboratory of the Rockies (NLR) at www.nrel.gov/publications.

We then tested whether the strains exhibited variations in alternative electron flow (AEF) pathways using the newly derived FRRf protocol in conjunction with well defined small molecule inhibitors of specific elements of different pathways governing the fates of electron energies. The plastid terminal oxidase (PTOX) pathway directly oxidizes plastoquinone pools, and its activity is inhibited by octyl gallate *in vivo*. The strong NPQ reduction in TG2 cells when challenged with OG (Fig. 2.4.A) indicated that the rapidly responsive PTOX mechanism contributes to the extremely high capacity to grow immediately upon high light exposure. However, PTOX has been shown to generate superoxide, making it a poor long term energy dissipation method. The antimycin A (AA) sensitive CEF pathway is a more sustainable solution to handling the excessive driving energy experienced by the photosynthetic electron transfer chain (PETC) apparatus under high light intensity, and contributed approximately half of the NPQ capacity exhibited by TG1-WT cells (Fig. 2.4.B), as observed by NPQ reduction in acclimated cells. The lack of this dynamic in TG2 and the TG2-CCA1 containing TG1-MYB99 call for an alternative explanation for their tolerance to large photon flux rates. This can reasonably be attributed to alterations in overall biochemistry that favors NADPH relative to ATP needs, which may speak to an overarching tendency for algal species to be more proteinaceous during rapid growth during which linear electron flow can be accelerated along with NADPH consumption and thereby pulling excessive energy out of the PETC.

This report is available at no cost from the National Laboratory of the Rockies (NLR) at www.nrel.gov/publications.

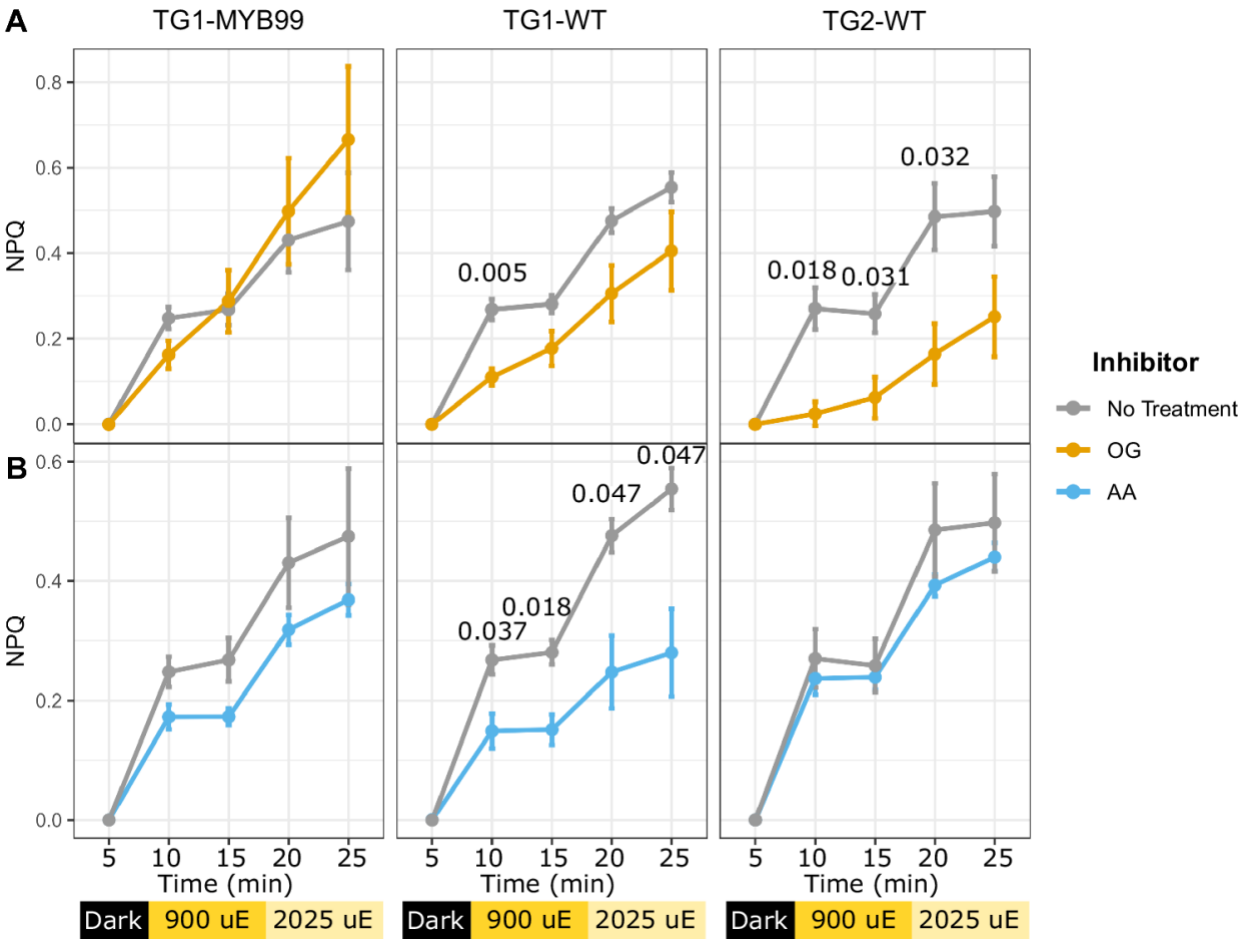

Fig. 2.4. Non-photochemical quenching (NPQ) responses of high light acclimated cell cultures. Replicate cultures were sampled and treated with inhibitors reported to interfere with different NPQ mechanisms including (A) octyl gallate (OG) and (B) antimycin A (AA). Data points are presented as mean values ± SD of biological replicate cultures (n = 3). Asterisks indicate significant differences between inhibitor treated NPQ measures and untreated control values as determined by a two-sided T-test, with p-values displayed above each significantly different comparison ($p < 0.05$) and insignificant p-values omitted

The outcome of task 1 and 2 were combined and reported in a high-impact (Nature Communications, impact factor 14.7) journal article (*1*) describing the fundamental photosynthetic underpinning of fast-growing algae and reported an identified central transcriptional regulator, which was demonstrated to increase the rate of carbon assimilation, productivity and biomass yield. For detailed experimental description and discussion, the reader is referred to the following published, Open Access, manuscript; https://www.nature.com/articles/s41467-024-49090-7.

This work directly addresses the fundamental questions on the molecular basis for growth rate determination may elucidate mechanisms that can be translated and tool development that can be ultimately transferred to species amenable to large-scale farming operations. Throughout this work, we continuously discussed commercialization opportunities and pursued intellectual property filings, with the team collectively deciding against IP protection on the engineered organisms (ref. team emails, 10/19/2021, NLR record of invention ROI-22-05).

This report is available at no cost from the National Laboratory of the Rockies (NLR) at www.nrel.gov/publications.

We were unable to analyze the CO_2 uptake between the two different cultivars as planned with the MIMS system, because the instrument was not functional at the time. The respective CO_2 assimilation rates were inferred from the metabolic flux studies that are presented in Figure 3 (as part of the discussion for task 2 activities). The detailed photophysiology experiments that were planned, were covered the respective cultivar response to different wavelengths of light, in the fast repetition-rate fluorometry (FRRf), described in Figure 4 and in supplementary information of the manuscript referenced above.

Task 3: Develop a detailed model of fluid mixing in open raceway ponds at scales relevant to outdoor algae cultivation, to understand the interaction of physical mixing of algae at production scales and the physiological response within the culture. To further understand the impact of changes to the physical mixing growth models will be developed that allow for rapid prediction in silico, and enable optimization of growth and carbon assimilation in outdoor-relevant conditions.

Planned activities:

- Develop and apply models to show how well mixed large raceway ponds are, identify the characteristics that could influence algal photophysiological response to the mixing, and identify potential approaches to improve productivity by changing the physical mixing by means that are consistent with economics of large-scale pond operation.
- Apply growth models incorporating fluid mixing to inform the efforts in task 2 on how to optimize light-driven biomass productivity and translate fundamental observations on photosynthesis efficiency and carbon assimilation to large-scale algae cultivation.

The outcome of task 3 will be an established, detailed, and shareable fluid dynamics model for standard raceway open algae pond mixing at scales relevant to algae farming for biofuels production, where operational parameters can be optimized computationally for maximum photosynthetic biomass productivity in a fluctuating light environment. Ultimately, this work will incorporate a highly granular algae growth model to expand the hypothesis testing dimensionality by computational experimentation beyond what is feasible in the laboratory.

Task 3 Results:

In order to test various cultivation configurations and help guide the design and future installation of large scale ponds, a dedicated task was devoted to building the simulation environment for computational fluid dynamics (CFD) modeling.

CFD models were developed and applied to show how well mixed large raceway ponds are, identify the characteristics that could influence algal photophysiological response to the mixing, and identify potential approaches to improve productivity by changing the physical mixing by means that are consistent with economics of large-scale pond operations.

This report is available at no cost from the National Laboratory of the Rockies (NLR) at www.nrel.gov/publications.

The design of the open raceway ponds used for these simulations is based the most common designs represented in the literature and uses a paddlewheel to circulate the water. The depth of typical ponds is between 15 and 40 cm, this allows for adequate light exposure, but depending on the climate conditions and the system configuration could promote water loses. Figure 1 shows the typical open raceway pond characteristics. The system described in this work is a 0.1 acre pond (14.2 m x 55 m) built in California USA. The pond was operated at 0.2 m water depth although other water depths are possible according to the seasons, walls of the reactor having a total height of 0.4 m. The reactor was built using a 1.5 mm polyethylene sheet arranged into the ground directly. The velocity of the paddlewheel was controlled by an inverter connected to an engine of 1.5 kW. Illustrations of the pond characteristics, configuration and computational mesh used are included in Figs. 3.1 and 3.2.

The flow dynamics in the pond requires an appropriate turbulence model to represent the different interactions between walls and paddlewheel and specifically requires specialized numerical algorithms to represent the motion and liquid phase interactions. The mathematical equations of motion and the computational framework used for their solution has been reported in a manuscript draft, and can be made available. The fluid dynamics of the system is captured by solving mass and momentum transport equations, that take into account the weighted contribution of density and viscosity of the liquid phase. A Stationary and a rotating mesh domain are used to allow for the relative motion between the paddlewheel and the water in the pond. The Arbitrary Mesh Interface (AMI) is used as a boundary condition to couple the flow between stationary and moving zones. To simulate the system we use the open-source CFD tool OpenFOAM version 8, with the interFoam solver, which is capable of solving unsteady, multiphase flow considering the rotational movement of the mesh domain around the paddlewheel. A constant pressure boundary condition is applied to the channel top surface which is open to the air. The channel walls and spokes of the paddles are defined as non-slip boundaries by specifying zero velocity in all directions. The set of mathematical equations essentially represent the volume of fluid (VOF) method, which is additionally coupled to a compression algorithm to prevent smearing of the phase fractions. The pond simulations were run using the HPC computational resources at NLR. Because of a significant computational resource requirement, we made computational approximations for the paddlewheel, and assumed that the velocity profiles could be used as velocity boundary conditions for a non-AMI mesh, which, when parameterized as periodic functions, can be used as the inlet boundary for the ponds (and reducing the computational burden by 5x).

This report is available at no cost from the National Laboratory of the Rockies (NLR) at www.nrel.gov/publications.

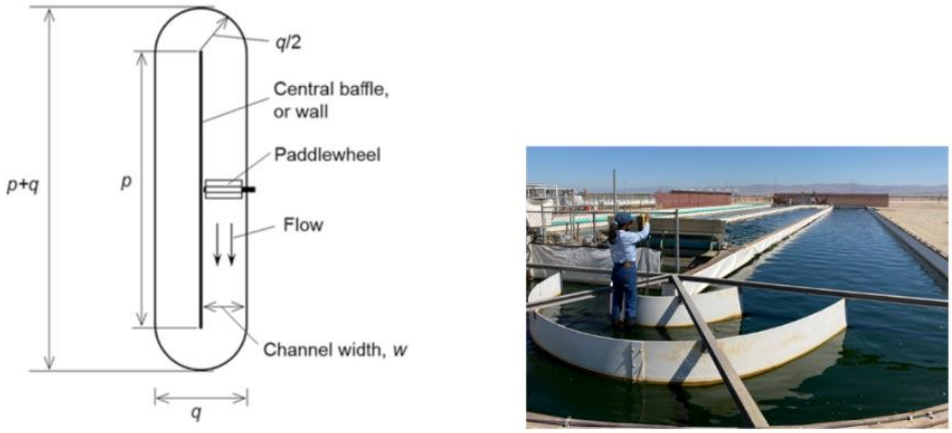

Fig. 3.1. Pond characteristics and general configuration

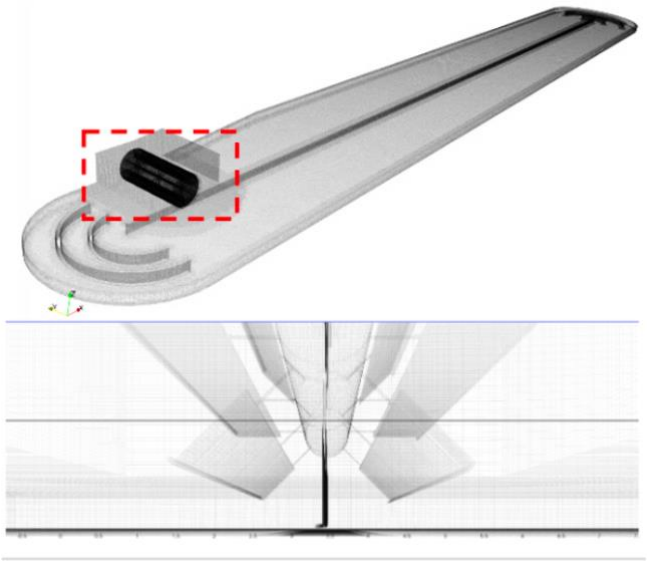

Fig. 3.2. Computational mesh illustration with a focus on the paddlewheel for fluid mixing.

To validate the computational models used in the simulation of the raceway ponds, we compared experimentally determined velocity profiles from operating 494 m2 raceway ponds and compared against the simulated and calculated velocity. The results for horizontal (along the channel) and vertical (perpendicular to the channel) velocities are shown relative to the origin locations from the dividing wall at the center of the pond (Fig. 3.3).

This report is available at no cost from the National Laboratory of the Rockies (NLR) at www.nrel.gov/publications.

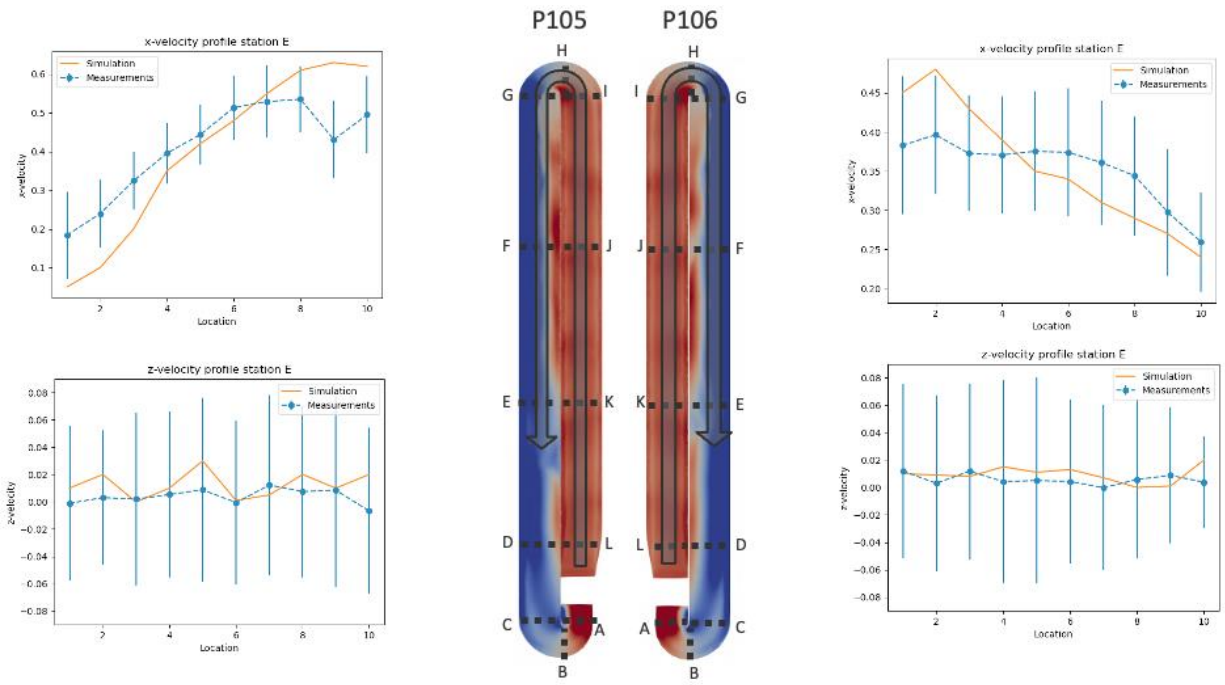

Fig. 3.3. Comparison of x-velocity (horizontal along the channels) and z-velocity (vertical mixing) profiles against experimental measurements for location E along the length of two operational raceway ponds at the Exxon-supported algae cultivation facility (California Advanced Algae Facility, CAAF, by Synthetic Genomics/Viridos, in Calipatria, CA). Left side is for the P105 reactor and the right side shows the P106 reactor.

The comparison of experimental and simulation results are shown, and indicate reasonable agreement and supports the use of the model for mixing simulation optimization. Some over prediction was noted on the horizontal velocity in the channel closest to the paddlewheel, which can be attributed to the approximate that was made to the rotating boundary. The vertical velocity (z) shows only small variations in the coordinates for both experiments and simulation. Mixing in the vertical direction is relevant to the dynamics of light exposure. More mixing is typically related to more efficient photosynthetic processes. While the simulations appear accurate in representing the vertical direction mixing, the overall mixing is poor, and suggest that most of the longitudinal movement of the algae suspensions are happening in a stratified laminar-like flow.

To improve vertical mixing, we tested the implementation of suspended baffles in the liquid phase, in the shape of delta wings. This approach has been reported before, where deflector baffles were added to the bottom of a small scale pond (10 m long, 0.93 m width per channel) to improve mixing (*6*) For the computational study here, we used 3x2.6” (LxW) delta wings, tilted 25 degrees facing the incoming flow upstream to the channel, and one array composed of 29 delta wings (Fig. 3.4). Initial analyses indicate that the vertical mixing at the location of the installed delta wings is increased relative to the baseline laminar flow (Fig. 3.5), with the higher turbulence assumed to increase light-access for the suspended algae particles.

This report is available at no cost from the National Laboratory of the Rockies (NLR) at www.nrel.gov/publications.

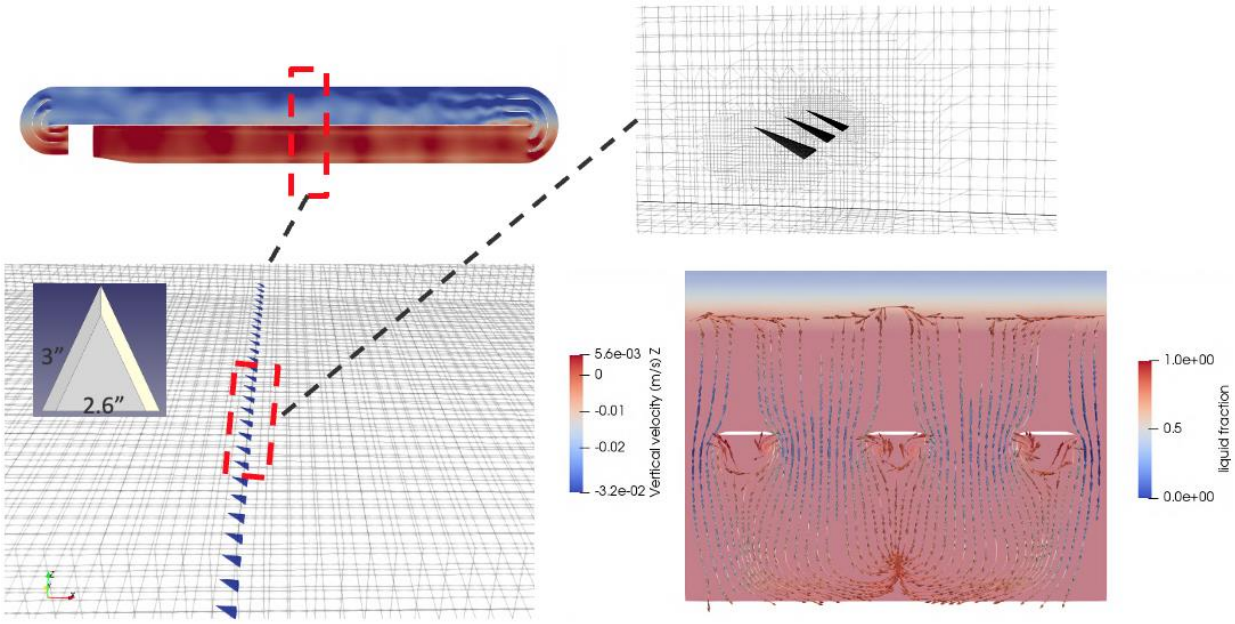

Fig. 3.4. Illustration of mesh details for the placement of delta-wings, suspended in a 14ft wide channel (fits 60 delta wings, separated at 3”). The mesh is refined 4x to capture the features and mixing parameters surrounding the suspended wings, for a small section of the channel the velocity profile is shown, illustrating increased mixing surrounding the suspended wings

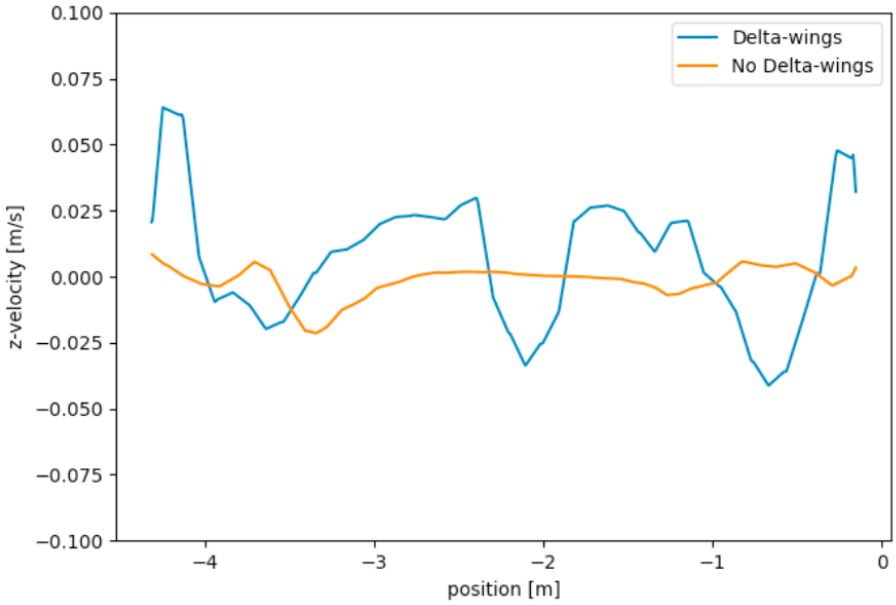

Fig. 3.5. Vertical velocity across the width of the pond as simulated without and with the delta wings in place

This report is available at no cost from the National Laboratory of the Rockies (NLR) at www.nrel.gov/publications.

To achieve the increased mixing with the delta wings, increased power is required to move water around the raceway pond. The turbulent dissipation (rate at which energy is dissipated in the system) is one metric that is considered an indicator of local turbulent, and enhances mixing, and is increased in the presence of the delta wings. The dissipation rate increases close to the array and decays rapidly thereafter, reaching up to 1.7X higher rates in the presence of the wings. Using the simulation CFD models, the head loss and drag loss for submerged bodies was calculated. Assuming a fixed paddlewheel rotation, a 17% increase in power is needed when the delta wings are installed, reaching approximately 0.175 W/m2 for the delta wings case, relative to an average of 0.15 W/m2 for the base case (for the 494 m2 cultivation ponds).

We were unable to apply algae growth models into the simulation of fluid mixing due to staff turn over and alternate priorities. This remains an important future area of development for algae production pond optimization. to inform the efforts in task 2 on how to optimize light-driven biomass productivity and translate fundamental observations on photosynthesis efficiency and carbon assimilation to large-scale algae cultivation.

Task 4: Techno-Economic Analysis (TEA) modeling for ExxonMobil process configuration

Planned activities:

NLR will modify its existing process/TEA models for both algae cultivation and conversion to reflect the process configuration as envisioned by ExxonMobil for commercial scale0up of algal biofuels technology concept (Figure 4.1). Namely, for cultivation this will entail updating the NLR models to reflect a larger farm scale (up to 20,000 acres), nutrient/CO2 inputs reflective of high-lipid, low-protein biomass compositions at final harvest, impacts for full pond liners, and all dewatering done via hollow-fiber membrane systems (versus NLR's three-stage dewatering process), as well as other modifications relative to NLR's published algae farm "design case" (https://www.nrel.gov/docs/fy16osti/64772.pdf). Likewise, for conversion this will entail modifying NLR's "Combined Algae Processing" (CAP) model framework (for example as published in https://www.nrel.gov/docs/fy14osti/62368.pdf) to reflect a more simplified processing schematic composed of wet cell disruption via steam lysis and lipid extraction/upgrading (hydrotreating) to hydrocarbon fuels, with the remaining extracted residual biomass sent to drying and sale for animal feed markets, e.g. as a soy meal replacement.

This report is available at no cost from the National Laboratory of the Rockies (NLR) at www.nrel.gov/publications.

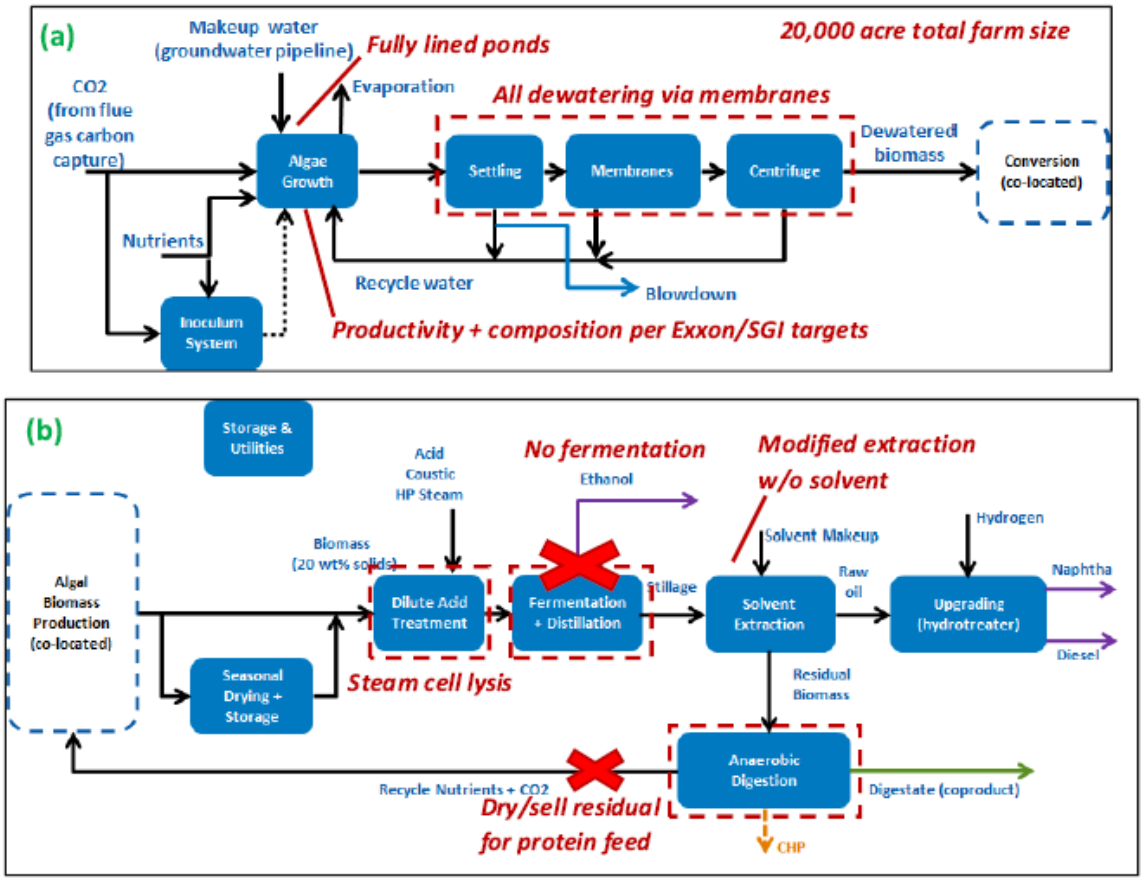

Fig. 4.1. Schematic diagrams depicting base-case NLR process configuration for algae production, harvesting and processing to fuels. (a) cultivation and harvesting operations, indication key modifications to base case assumptions on farm size and pond configuration and dewatering operations, (b) conversion operations, with key modifications indicated in red.

Task 4 Results:

As part of this task 4 effort, techno-economic analysis (TEA) modeling was conducted to estimate key economic metrics including minimum biomass selling price, minimum fuel selling price, and conversion processing internal rate of return (IRR) based on exercising NLR's TEA models for algal biomass production and conversion to fuels (*7*, *8*), modified to reflect Exxon/SGI-envisioned process targets for a future nth-plant 10,000 bbl/day commercial facility scale. Figure 4.1 indicates the baseline cultivation model (a) and the process modifications specifically requested by Exxon for this analysis for the downstream conversion.

This report is available at no cost from the National Laboratory of the Rockies (NLR) at www.nrel.gov/publications.

The results from the analysis calculated the modeled minimum fuel selling price (MFSP) for a base case scenario maximizing diesel fuel output, increasing to $4.39/gal for an alternate scenario maximizing jet fuel production, in both cases based on a targeted strain performance projected to achieve exceptionally high cultivation productivity rates (31 g/m^2/day annual average biomass productivity) and lipid content (80% ash-free lipid composition = 25 g/m^2/day lipid productivity) coupled with a simple conversion process focused on lipid recovery and upgrading to fuels. Total capital investment for the integrated facility was estimated at roughly $4.6 billion for the max diesel case, or $4.9 billion for the max jet case associated with an additional hydrocracking step, with the majority of the costs for either case attributed to biomass production/harvesting at $3.8 billion. These MFSP estimates include a number of renewable fuel policy credit factors as may be supported when the analysis was carried out (October 2021) or in the near-future, without which the MFSPs would increase to $6.07/gal and $6.81/gal for the respective cases (this represents a key difference from prior NLR models which historically have not assumed policy credit inclusions, but instead required pursuing more costly and complex biorefinery configurations to produce high-value coproducts as an alternative means of reducing MFSPs). Sensitivity analysis scenarios are also presented highlighting impacts to both cultivation and conversion economics across a number of alternative conditions/performance levels.

As typical for algal biomass production, the production ponds constitute the largest contribution to the MBSP, driven in turn by capital expenses (Fig 4.2),Fig however, this contribution is somewhat diminished relative to NLR's standard TEA models given the use of larger 20-acre ponds assumed here (though this is outweighed by higher expenses with full pond liners). The second-largest contributor is from CO_2 and nutrient costs, the large majority (97%) of which is driven by CO_2 given the high C and low N/P content of the biomass assumed here. Dewatering also constitutes a large share of the MBSP contribution, reflective of the use of membranes for primary (and only) dewatering which are considerably more costly per volume throughput than the NLR basis model assumption with primary gravity settling (though recognizing gravity settling is both strain- and composition-dependent and may not be practical for this situation). Inoculum, CO_2 storage, and water circulation pipelines all make up a relatively small contribution to system costs, although as discussed with Exxon/SGI, the latter for water circulation may be smaller than the Exxon/SGI costs because water circulation is achieved in part through lower-cost aqueduct-style troughs than pipelines for moving water in downhill directions.

This report is available at no cost from the National Laboratory of the Rockies (NLR) at www.nrel.gov/publications.

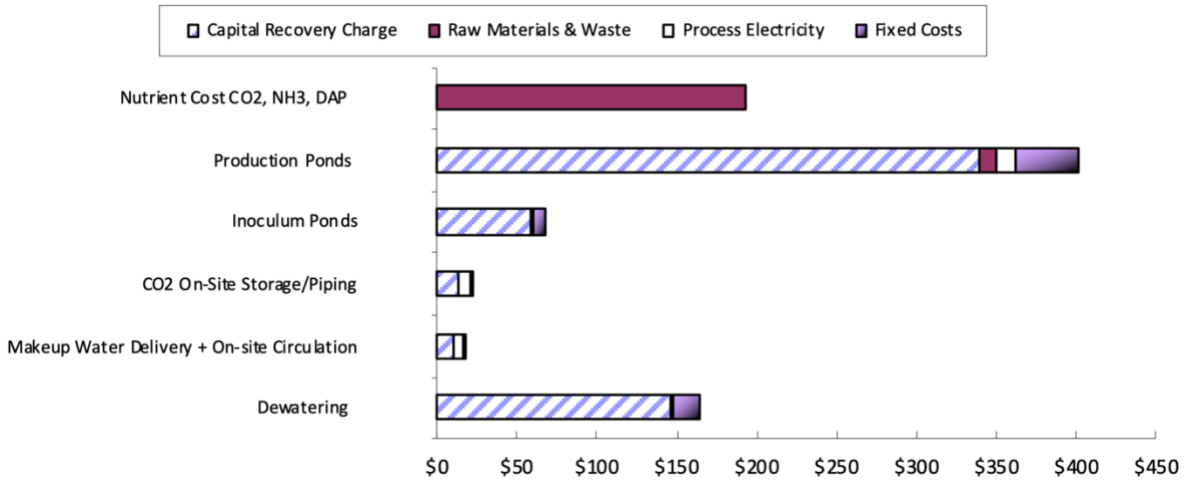

Fig. 4.2. Cost breakdown for the cultivation facility base case model, shown as respective contribution to the cost of one dry ton of biomass, minimum biomass selling price (MBSP).

Capital costs for the conversion facility are significantly lower than the cultivation facility, but still make up a sizeable portion of the total capital investment (17%-23%). This can also be seen in the cost breakdown of the conversion facility (Fig. 4.3), where all costs associated with the cultivation facility are lumped into "feedstock cost," which dominates all other process costs. Capital costs for the conversion facility are strongly driven by the drying equipment, specified as a double drum dryer. Based on previous communication with equipment vendors, the scale-up of this equipment is fairly limited; thus, a large number of individual dryers are required to meet the demands of the process, resulting in a significant cost inefficiency. Alternative drying methods that are more scalable may yield economic benefits but may also be unsuitable for the unique rheology of algal biomass. Capital costs for the product upgrading section are also fairly significant, especially for the "max jet" case, which requires an additional hydrocracking step. These additional equipment costs are the primary cost driver for the increased MFSP of the max jet case. A lower overall fuel yield and an increased proportion of naphtha also has a minor negative influence on economics compared to the base case.

For both cases, coproducts and policy credits play a key role in providing supplemental revenue for the biorefinery; however, fuels are the primary product, making up over half of the revenue in each case given very high fuel yields from the substantial lipid fraction of the biomass. Dried solids are sold at $400/ton, accounting for approximately 12% of the revenue for the biorefinery. Policy credits play an even greater role. RINs and the generic low-emissions fuel policy make up approximately 30% of revenue, with the remainder of the "revenue" attributed to a credit for CO_2 recycled back to the cultivation ponds, reflecting raw material savings for the biomass cultivation.

This report is available at no cost from the National Laboratory of the Rockies (NLR) at www.nrel.gov/publications.

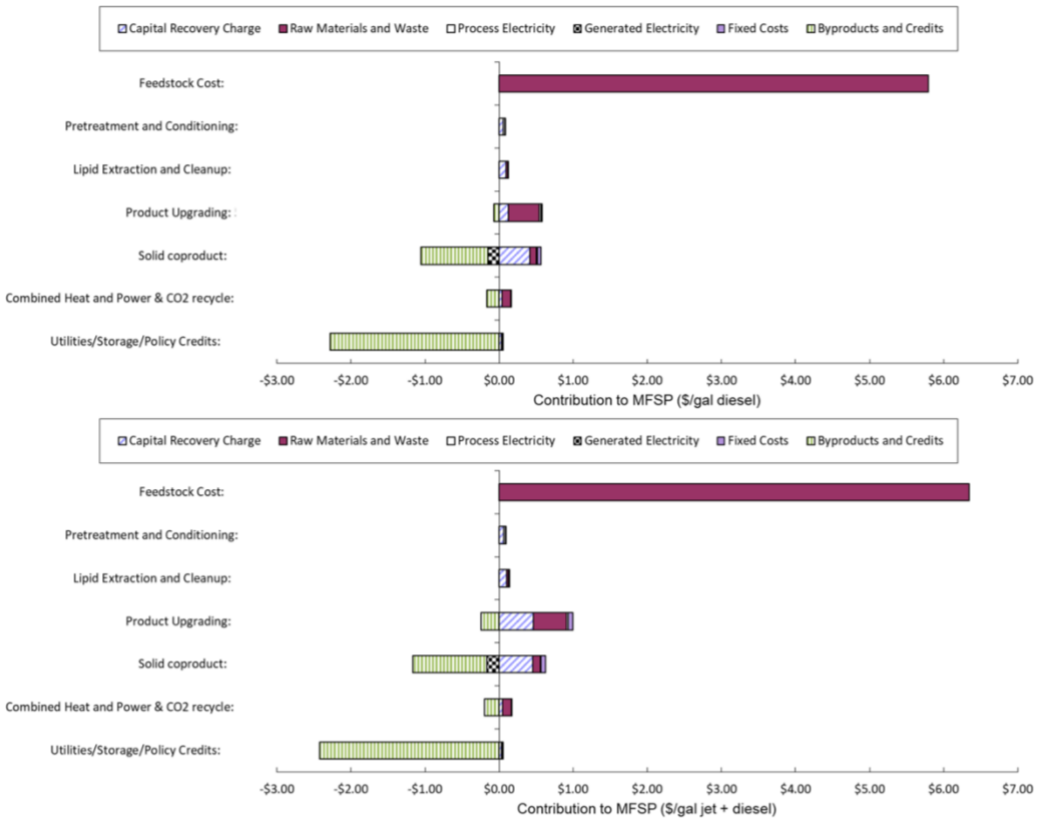

Fig. 4.3. Cost sensitivity breakdown for the conversion facility for the base case (top) and the max jet case (bottom).

Task 5: Feasibility cost estimation for pilot-scale facility buildout.

Planned activities:

NLR will exercise existing cost-estimates currently in-hand for scaled-down algae ponds and other unit operations constituting pilot-scale facility sizes producing 2, 5, and 50 bbl/day of extracted lipid biocrude (three scale scenarios). NLR has not procured, built, or operated algae ponds, and thus cannot provide direct guidance on what such ponds may cost ExxonMobil to construct as part of the above-noted pilot scale scenarios; however, NLR has received a number of vendor/contractor-supplied cost estimated for a range of algae pond sizes and designs, which would be the basis for the analysis to be conducted here. Accordingly, as discussed with ExxonMobil, this task would primarily consist of comparing existing cost estimates that ExxonMobil and NLR have already established as may be applicable to facility scales spanning the above ranges, without seeking any new cost estimates (the latter most appropriately would require working with similar vendors/subcontractors as NLR has done in the past in order to establish more tailored cost quotations). Up to three pond design cost estimates will be considered, selecting one as the most appropriate to the selected scale scenario, with downstream operations (dewatering, conversion pretreatment/extraction/residual drying) to be scaled down from original quotations.

This report is available at no cost from the National Laboratory of the Rockies (NLR) at www.nrel.gov/publications.

Task 5 Results:

To support the feasibility assessment of a pilot-scale facility buildout, capital and operating cost estimates were established for key unit operations including cultivation, dewatering, and drying for three pilot plant expansion scenarios as may be deployed in a more near-term timeframe, spanning 2.5 and 5 bbl/day scales reflective of a brownfield expansion of current pilot plant infrastructure, as well as a separate 50 bbl/day greenfield pilot plant option. The capital costs for all scenarios under both tasks were based on extrapolations from vendor/subcontractor inputs furnished previously to NLR in support of TEA design case publications over recent years, as the scope did not include establishment of any "new" design/cost estimates.

The results of this analysis yielded fixed capital investment estimates of $6MM and $10MM for the 2.5 and 5 bbl/day scales, respectively (the latter representing $4MM incremental additional costs assuming the pilot plant facility were first expanded to 2.5 bbl/day), when assuming Exxon-furnished guidance for indirect capital cost factors, and extrapolations from vendor and subcontractor-furnished figures. The associated variable operating costs were estimated at roughly $140,000/yr for the 2.5 bpd case or $240,000/yr for the 5 bpd case (these figures do not include labor or any other fixed operating expenses). For the separate 50 bpd greenfield design, fixed capital investment expenses were estimated at $28MM and $34MM for either membrane or centrifuge-based dewatering options, while variable operating costs were estimated at $2.2 MM/yr. These expenses for all three scales are inclusive of cultivation, dewatering, and biomass drying; separately, cost estimates for a dry lipid extraction unit were considered based on published details outside of NLR in-house information, with installed capital costs estimated at $400,000, $600,000, and $2.4MM for the 2.5, 5, and 50 bpd scales, respectively, and with variable operating costs estimated at roughly $50,000/yr, $100,000/yr, and $1MM/yr for the three respective scales.

To illustrate the impact of size of the algae cultivation facility, Fig. 5.1 shows the total estimated costs (direct and indirect) to build the pilot plants in question. Depending on the assumptions for the calculation of indirect costs, expanding the facility size up to 2.5 bbl/day capacity or 5 bbl/day would require additional incremental capital investment costs.

This report is available at no cost from the National Laboratory of the Rockies (NLR) at www.nrel.gov/publications.

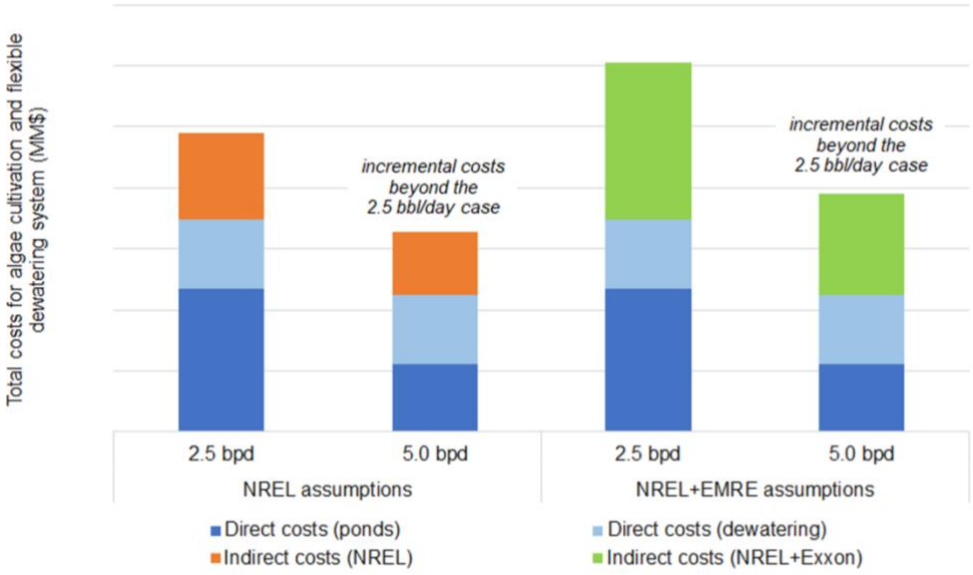

Fig. 5.1. Total direct and indirect costs distribution for the full 2.5 and 5 bbl/day facilities, comprising algae cultivation and a flexible dewatering system.

The completed preliminary economic analysis/TEA modeling for future n^{th}-plant projections around a 10 kbd aspirational algal biofuel facility as well as supplying capital/operating cost estimates for three small-scale pilot plant scenarios as may be deployed in the near-term, is briefly summarized here and was reported in great detail in a technical report delivered to Exxon in October 2021. The reported figures translate to MFSP estimates of $3.78/gal and $4.39/gal for the max diesel and max jet scenarios, respectively, which would increase to $6.07/gal and $6.81/gal for the respective cases without the inclusion of any policy incentive credits – thus highlighting a key factor here in the influence such policy credits impart on overall system economics, though also allowing for greatly simplifying the conversion process relative to configurations recently evaluated by NLR reflecting more complex and costly processing trains including higher-value coproducts otherwise required to achieve MFSP goals.
We stress that the cost/TEA values furnished here under the analysis tasks as described here are best viewed as feasibility-level estimates akin to AACE Class 4 engineering design, although they pull from what we feel to be credible and well-informed vendor/subcontractor inputs well exceeding the level of fidelity that would be possible through standard cost databases or independent engineering cost estimation methodologies.

This report serves to meet the requirement for the CRADA Final Report with preparation and submission in accordance with the agreement's Article X.

This report is available at no cost from the National Laboratory of the Rockies (NLR) at www.nrel.gov/publications.

References:

1. Steichen, Seth, Arnav Deshpande, Megan Mosey, Jessica Loob, Damien Douchi, Eric Knoshaug, Stuart Brown, Robert Nielsen, Joseph Weissman, L. Ruby Carrillo, and Lieve Laurens. 2024. "Central transcriptional regulator controls photosynthetic growth and carbon storage in response to high light." Nature Communications 15, 4842 https://doi.org/10.1038/s41467-024-49090-7

2. Krishnan, Anagha, Maria Likhogrud, Melissa Cano, Scott Edmundson, Jenna B. Melanson, Michael Huesemann, John McGowen, Joseph C. Weissman, and Matthew C. Posewitz. 2021. "Picochlorum celeri as a model system for robust outdoor algal growth in seawater." Scientific Reports 11, 1–13. https://www.osti.gov/biblio/1785572

3. Weissman, Joseph C., Maria Likhogrud, Dylan C. Thomas, Wei Fang, Devin A.J. Karns, Jeffrey W. Chung, Robert Nielsen, and Matthew C. Posewitz. 2018. "High-light selection produces a fast-growing Picochlorum celeri. Algal Research 36, 17–28. https://doi.org/10.1016/j.algal.2018.09.024

4. Liang, Feiyan, and Peter Lindblad. 2016. "Effects of overexpressing photosynthetic carbon flux control enzymes in the cyanobacterium Synechocystis PCC 6803." Metabolic Engineering 38, 56–64. DOI:10.1016/j.ymben.2016.06.005

5. Allen, Douglas K., IGOR G. L. LIBOUREL, and Yair Shachar-Hill. 2009. "Metabolic flux analysis in plants: coping with complexity." Plant, Cell and Environment 32, 1241–1257. DOI:10.1111/j.1365-3040.2009.01992.x

6. Amanna, Behnam, Parisa A. Bahri, and Navid R. Moheimani. 2015. "Investigation on the performance of raceway ponds with internal structures by the means of CFD simulations and experiments." Algal Research 10, 64–71. https://doi.org/10.1016/j.algal.2024.103718

7. Davis, Ryan, Jennifer Markham, Christopher Kinchin, Nicholas Grundl, Eric C.D. Tan, David Humbird. 2018. “Process Design and Economics for the Production of Algal Biomass: Algal Biomass Production in Open Pond Systems and Processing Through Dewatering for Downstream Conversion.” Algal Research Volume 36, Pages 17-28. https://doi.org/10.2172/1239893

8. Davis, Ryan, Christopher Kinchin, Jennifer Markham, Eric C.D. Tan, Lieve Laurens, D. Sexton, D. Knorr, P. Schoen, J. Lukas. 2014. “Process Design and Economics for the Conversion of Algal Biomass to Biofuels: Algal Biomass Fractionation to Lipid- and Carbohydrate-Derived Fuel Products”. Golden, CO: National Renewable Energy Laboratory NREL/TP-5100-62368. http://www.nrel.gov/docs/fy14osti/62368.pdf

Journal Article

Steichen, Seth, Arnav Deshpande, Megan Mosey, Jessica Loob, Damien Douchi, Eric Knoshaug, Stuart Brown, Robert Nielsen, Joseph Weissman, L. Ruby Carrillo, Lieve Laurens. 2024. “Central transcriptional regulator controls photosynthetic growth and carbon storage in response to high light.” Nature Communications 15, 4842. https://www.nrel.gov/docs/fy24osti/88146.pdf

This report is available at no cost from the National Laboratory of the Rockies (NLR) at www.nrel.gov/publications.

Subject Inventions Listing:

None.

ROI#:

ROI-23-97 *Algae and plant regulatory control elements enhancing carbon,* Laurens, Lieve; Steichen, Seth; Deshpande, Arnav, filed 6/7/2023

ROI-22-05 *Increased growth, yield, light response and CO2 assimilation rates in photosynthetic organisms*, Laurens, Lieve; Steichen, Seth; Shanta, Peter; Mosey, Megan; Knoshaug, Eric

This report is available at no cost from the National Laboratory of the Rockies (NLR) at www.nrel.gov/publications.